2010

Experimental Studies on the Plasma Bullet Propagation and Its Inhibition

Erdinc Karakas

Mounir Laroussi
Old Dominion University, mlarouss@odu.edu

Original Publication Citation

Karakas, E., & Laroussi, M. (2010). Experimental studies on the plasma bullet propagation and its inhibition. *Journal of Applied Physics, 108*(063305), 1-6. doi: 10.1063/1.3483935

AIP Journal of Applied Physics

Experimental studies on the plasma bullet propagation and its inhibition

Erdinc Karakas and Mounir Laroussi

Citation: Journal of Applied Physics **108**, 063305 (2010); doi: 10.1063/1.3483935
View online: http://dx.doi.org/10.1063/1.3483935
View Table of Contents: http://scitation.aip.org/content/aip/journal/jap/108/6?ver=pdfcov
Published by the AIP Publishing

Experimental studies on the plasma bullet propagation and its inhibition

Erdinc Karakas[a] and Mounir Laroussi[b]
Laser and Plasma Engineering Institute, Old Dominion University, Norfolk, Virginia 23529, USA

(Received 10 May 2010; accepted 29 July 2010; published online 24 September 2010)

Plasma bullets generated by atmospheric pressure low temperature plasma jets have recently been an active research topic due to their unique properties and their enhanced plasma chemistry. In this paper, experimental insights into the plasma bullet lifetime and its velocity are reported. Data obtained from intensified charge-coupled device camera and time-resolved optical emission spectroscopy (OES) elucidated the existence of a weakly ionized channel between the plasma bullet and its source (such as the plasma pencil). Factors responsible for the inhibition of the propagation of the bullet, such as low helium mole fraction, the magnitude of the applied voltage, and the secondary discharge ignition time, are also revealed. A new technique is discussed to accurately measure the plasma bullet velocity, using time-resolved OES. This new technique shows that during its lifetime the plasma bullet goes through launching, propagation, and ending phases. In addition, it is noted that the plasma bullet exhibits an unstable behavior at the early beginning and late ending of the propagation. © *2010 American Institute of Physics*. [doi:10.1063/1.3483935]

I. INTRODUCTION

Atmospheric pressure low temperature plasma jets (APLTPJs) driven by very short pulses are of interest in various applications. Especially, their enhanced plasma chemistry has initiated a new era with marked technological impact in biomedical applications.[1,2] However, most of their physical properties are still not well-understood. Several experimental results have shown that the APLTPJs are not continuous media; the jet consists of a train of bulletlike structures (called plasma bullets), propagating in the surrounding air with supersonic velocities in the order of 10^4-10^5 m/s without any externally applied electric field.[3,4]

The interesting properties of the APLTPJs have increasingly attracted attention of several groups in recent years. However, most studies up to date are related to some basic characterizations such as voltage-current characteristics and emission spectra identifications. Only few works produced detailed studies of the physical and chemical characteristics of the APLTPJs.[3–7]

In this study, an APLTPJ reactor, the Plasma Pencil, is used. This device is made of a 25 mm diameter hollow dielectric tube with two copper ring electrodes attached to the surface of centrally perforated dielectric disks separated by 5 mm. The diameter of the hole is about 3 mm. The diameter of the copper ring electrodes is smaller than that of the disk but larger than that of the hole. In order to generate the plasma plume/jet/bullet, a unipolar square high voltage pulse in the order of 4.0 to 7.5 kV is applied to the electrodes with a pulse width (200 ns to several microseconds), a repetition rate up to 10 kHz, and a helium flow rate between 1 and 7 l/min. The high voltage pulse generation system includes a high voltage power supply (Spellman SL 1200, max. power: 1200 W), a high voltage pulse generator (DEI PVX-41, maximum output voltage: 10 kV), and a single channel arbitrary function generator (Tektronix AFG 3021). The gas flow into the reactor is controlled by a mass flow meter (Bronkhorst High-Tech). The optical emission spectroscopy (OES) system is composed of a monochromator (Acton Research Spectra 500-i), a photomultiplier tube (PMT) (Acton Research PD-471), lenses, and filters. In order to monitor the temporal evolution of the reactive species along the plasma jet, the output of the PMT is directly connected to 1 GHz wideband digital oscilloscope (Tektronix 784D) after adjusting the grating position of the monochromator. The images of the plasma bullet are taken by an intensified charge-coupled device (ICCD) camera (Cooke Corp., Dicam-Pro). The experimental setup is shown in Fig. 1.

The main aim of this paper is to determine the plasma bullet lifetime and its velocity as a function of different operating conditions. Note that the plasma bullet lifetime is related to the plasma jet length since the plasma jet is the footprint of the plasma bullets (i.e., if the plasma bullet travels to further distances, the plasma jet appears longer).

II. PLASMA BULLET LIFETIME

The plasma bullet lifetime depends on the helium mole fraction along the propagation path, the magnitude of the

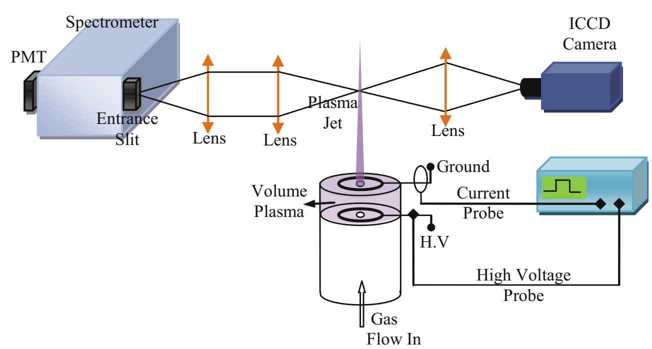

FIG. 1. (Color online) Experimental setup showing diagnostics consisting of a monochromator, an ICCD camera, and an oscilloscope. The light emitting from the plasma jet is collected by lenses.

a)Electronic mail: ekara002@odu.edu.
b)Electronic mail: mlarouss@odu.edu.

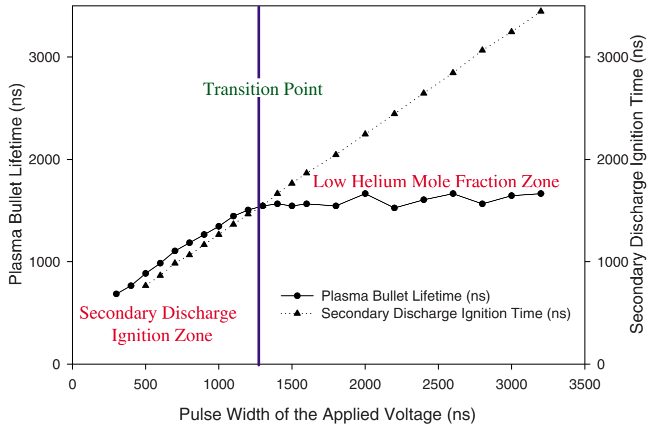

FIG. 2. (Color online) Plasma bullet lifetime as a function of the pulse width (applied voltage: 4 kV; repetition rate: 5 kHz; flow rate: 5.0 l/min).

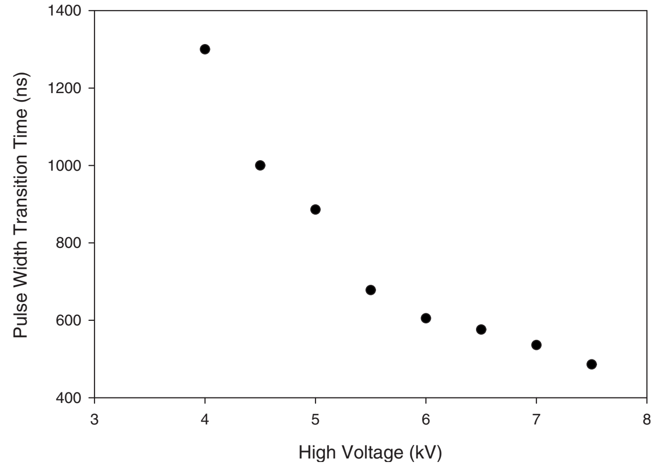

FIG. 3. The pulse width transition time as a function of the applied voltage (repetition rate: 5 kHz; flow rate: 5.0 l/min).

applied voltage, and the secondary discharge ignition time. In dielectric barrier discharge (DBD) sources that are driven by short high voltage pulses, Laroussi *et al.*[8] showed that in addition to the main discharge a secondary discharge is self-ignited during the fall-time of the applied high voltage pulse. The secondary discharge occurs at the end of the applied high voltage pulse due to the charge accumulation established by the primary main discharge on the surface of the dielectric.[8]

For a pulse width less than a certain value, the plasma bullet stops propagating just after the secondary discharge ignition. The reason for this interesting phenomenon will be investigated later in this paper. The ionization channel contains short-lived, such as He^*, N_2^*, N_2^+, and long-lived, such as He^m (helium metastables), O_3, NO, NO_2, reactive species. The zones, where the propagation of the plasma bullet is inhibited by low helium mole fraction or secondary discharge ignition, are shown in Fig. 2. If the pulse width is long enough, the plasma bullet propagation is inhibited before the ignition of the secondary discharge due to quenching by air molecules (mostly by oxygen) diffusing into the ionization channel. This limit is called the transition point that separates the plasma bullet inhibition zones (the secondary discharge ignition zone from low helium mole fraction zone) as seen in Fig. 2. This transition point shifts as a function of the applied voltage from 1300 to 425 ns (Fig. 3) since the plasma bullet is able to arrive to this transition point earlier at higher applied voltages due to its higher velocity.

This transition point is important for the optimum operating conditions of the plasma pencil. How the plasma bullet comes to an end affects the structure of the tip of the plasma plume. If the secondary discharge ignition inhibits the propagation of the plasma bullet, the plasma plume tip is shaped as a sharp and homogenous structure. In contrast, in the case of low helium mole fraction, the plasma jet tip seems inhomogeneous and is unstable. In applications, such as material processing or biomedicine, the condition of the tip of the plasma plume is very important since it is the part that comes in contact first with the surface under treatment.

A. Helium mole fraction and applied voltage

To sustain the plasma bullet propagation a minimum density of helium atoms is required in the propagation channel. This amount can be quantitatively represented by the helium mole fraction. The helium flow passing through the electrodes controls the length and homogeneity of the plasma jet. A correlation study between the plasma jet length and the helium mole fraction as a function of the helium flow velocity and applied voltage was reported in Ref. 9. The plasma jet length for different helium flow velocities was first measured, and then the minimum corresponding helium mole fraction at the tip of the plasma jet was extracted from the helium flow simulation results. This simulation was performed by a commercially available partial differential equation solver (COMSOL MULTIPHYSICS 3.4). Another factor, the magnitude of the applied voltage (the applied energy), was also presented. How much applied voltage is needed to initiate the plasma bullet formation (i.e., how much energy is transferred into the ionization channel) is an important parameter because the plasma bullet dissipates its energy as it propagates forward. In this study,[9] it was found that the helium mole fraction and applied voltage should be more than a critical value along the plasma bullet propagation path to sustain the plasma chemistry in the plasma bullets.

B. Secondary discharge ignition

As the plasma bullet propagates further, it leaves behind an ionization channel consisting of short-lived and long-lived reactive species. This is supported by ICCD camera photographs shown in Fig. 4 and temporal OES data shown in Fig. 5.

Our current experimental setup allows identifying only emitting species associated with short-lived species along the ionization channel. The temporal evolution of the emitting species provides an insight into the constituents of the channel. During the experiments, the focal point of our lens is 20 mm away from the plasma pencil. Basically, as the plasma bullet passes through this focal point, the distribution of the emitting species is recorded by the monochromator. As shown in Fig. 5, the magnitude of the emission intensity first increases and eventually reaches its highest value. This region corresponds to the point where the ionization front propagates forward. Then, the emission decreases exponen-

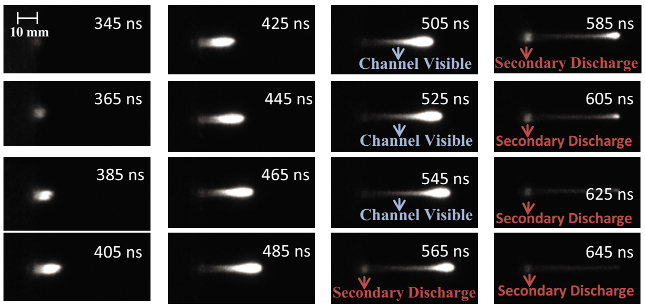

FIG. 4. (Color online) The plasma bullet propagation showing the channel consisting of emitting species along the ionization channel. Secondary discharge ignition causing the plasma bullet inhibition (applied voltage: 5.5 kV; pulse width: 300 ns; repetition rate: 5 kHz; flow rate: 5.0 l/min).

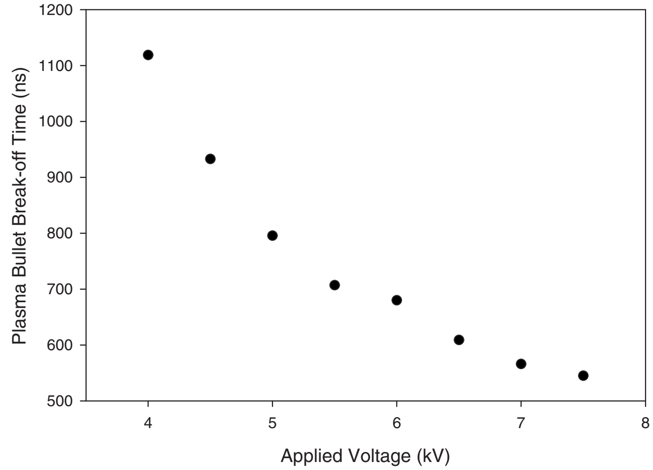

FIG. 6. Plasma bullet break-off time for different applied voltages (pulse width: 2000 ns; repetition rate: 5 kHz; flow rate: 5.0 l/min).

tially until it reaches low emission levels. This proves that even though the ionization front moves 50–60 mm away from the plasma pencil, it leaves behind short-lived reactive species which remain at low concentration values along the ionization channel.

The channel initially appears as an extension of the plasma bullet. If the applied voltage is sufficiently high, the plasma bullet eventually breaks off this extension. The time when the plasma bullet breaks off is determined as a function of the applied voltage. This break-off time corresponds to a point when the short-lived reactive species are at very low concentrations making them invisible to the ICCD camera (the ICCD camera can track emissions between 200 and 900 nm wavelengths). It is found that the plasma bullet breaks off faster at higher voltages (Fig. 6). This is due to the faster velocity of the plasma bullet at higher voltages.[4] However, this break-off time is independent of the pulse width.

Even when the plasma bullet breaks off, the secondary discharge ignition (initially occurring inside the device) is still able to inhibit the propagation of the plasma bullet. This supports the idea that long-lived species exist throughout the ionization channel along with low concentrations of short-lived species, which helps the outward expansion of the secondary discharge. Therefore, the secondary discharge initially ignited at the dielectric electrode surface propagates along the ionization channel, and then stops the plasma bullet from propagating in an abrupt manner. In order to observe the secondary discharge propagation, the operating conditions of the plasma pencil are set to 7 kV applied high voltage and 2800 ns pulse width, which allow for an easy observation of the secondary discharge during its propagation. In addition, the 2800 ns pulse width provides for a good separation of this propagation from that of the plasma bullet, and eliminates the contribution of the short-lived species along the ionization channel.

Figure 7 shows that the secondary discharge also travels in the air up to 40 mm away from the reactor. Therefore, it is deduced that the secondary discharge ignition creates another propagation in the surrounding air.

The secondary discharge effect on the plasma bullet inhibition can be explained by our recent experimental observations. Based on these observations, it is confirmed that the plasma bullets adopt the streamer propagation mechanism as was proposed in Ref. 3. These observations show that the plasma bullets generated by positive applied voltages travel similarly as in the case of the cathode-directed streamers. In this streamer mechanism, the electron flow is opposite to the direction of propagation of the plasma bullet. It is also found that during the propagation a number of the electrons accumulate onto the positive electrode dielectric surface. The electron number in this accumulation is almost equal to the electron number in the plasma bullet. When these electrons are released from the dielectric surface at the end of the

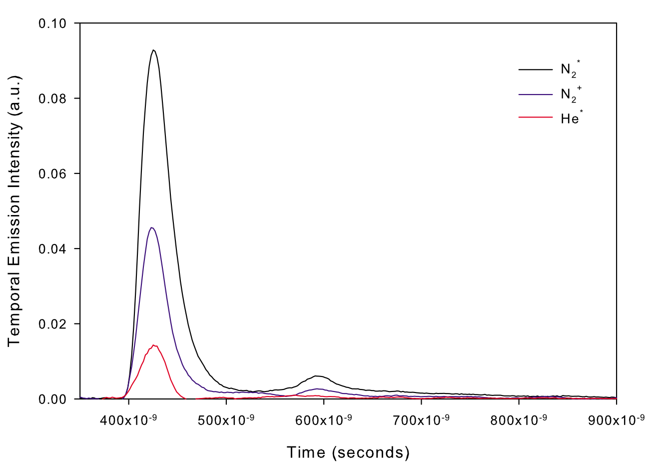

FIG. 5. (Color online) Temporal evolution of the reactive species at 20 mm away from the plasma pencil (applied voltage: 5.5 kV; pulse width: 1000 ns; repetition rate: 5 kHz; flow rate: 5.0 l/min).

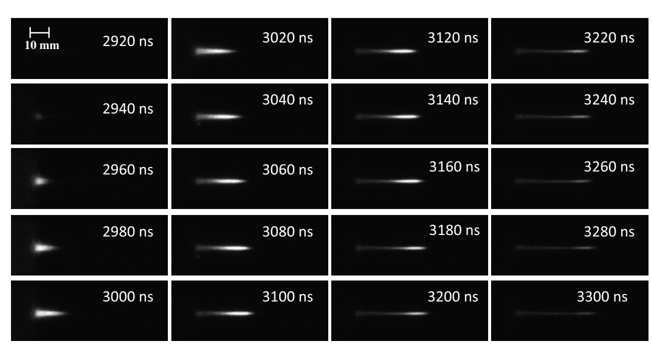

FIG. 7. Secondary discharge propagation at 7 kV applied voltage and 2800 ns pulse width.

applied voltage pulse, they create an opposing current along the ionization channel. Therefore, this "negative current," acting against the normal succession of events during the bullet propagation, leads to slowing down of the plasma bullet and then eventually its inhibition. This mechanism needs further detailed investigations and will be reported in a future publication.

III. ACCURATE MEASUREMENT OF THE PLASMA BULLET VELOCITY BY OES

Measurement of the plasma bullet velocity is an important and necessary task for the investigations of the dynamics of the plasma bullet propagation. In several studies,[3,4,10,11] the plasma bullet velocity is measured using ICCD camera images. High-speed photography based on the ICCD cameras allows observing the plasma dynamics in time domain with resolutions as low as a few nanoseconds. Even though this technique is unique, the resolution of the ICCD cameras is not high enough for the plasma bullet velocity to be measured in detail.

In our previous work, the instantaneous plasma bullet velocity was determined by an ICCD camera with a resolution of 20 ns.[4] This resolution is not enough to elucidate the detailed behavior of the plasma bullet during its propagation in the surrounding air. In previous work, it was reported that the plasma bullet starts its propagation with relatively lower velocities, and then it reaches its maximum. As it travels further, its velocity decreases. Finally, at the end of the applied voltage pulse, the plasma bullet stops propagating. Unfortunately, fluctuations in the instantaneous plasma bullet velocity plagued the measurements in that study.

Although the resolution of the ICCD cameras could be as low as 3 ns in theory, an exposure time of around 20 ns is usually needed to collect a sufficient amount of photons in order to observe the plasma bullet. In addition, a precise protocol is necessary to identify a reference point in order to measure the distance from the plasma bullet to the reactor. This rendered the task particularly difficult and required the use of advanced image processing technique.

In the present study, a time-resolved OES is applied to the measurement of the plasma bullet velocity with a resolution as good as 0.5 ns. Figure 5 shows the temporal evolution of the reactive species at 20 mm away from the plasma pencil for the applied voltage of 5.5 kV with a 1 μs pulse width. Spectral lines for these reactive species are as follows: N_2^* [second positive system (SPS)]: 337.1 nm line of C $^3\Pi_u \rightarrow$ B $^3\Pi_g$, N_2^+; (first negative system): 391.4 nm line of B $^2\Sigma_u^+ \rightarrow$ X $^2\Pi_g^+$, and He*: 706.5 nm line. The chosen lines are determined in terms of the magnitude of emissions in their spectral systems.

Based on Fig. 5, the reactive species emit their highest peaks at around 425 ns. The occurring time of these peaks depends on the magnitude of the applied voltage and the focusing position of the lenses along the plasma jet. For example, at further spatial points the highest peak occurs later, or with higher applied voltages the highest peak occurs earlier. The former is illustrated in Fig. 8. In this technique, these shifts will be basically utilized for the measurement of the plasma bullet velocity.

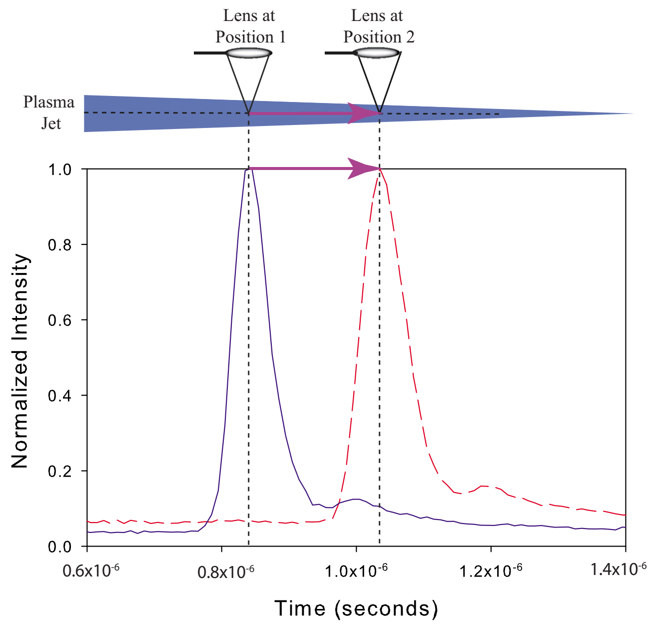

FIG. 8. (Color online) Showing a shift in the highest emission peak for the plasma bullet velocity measurements.

The average and instantaneous plasma bullet velocities are measured from the temporal evolution of the reactive species. The emitted light is collected along the plasma jet, and is monitored on a wideband oscilloscope. The time that the plasma bullet propagates in the air (i.e., time of the highest peak of the reactive species emission) is measured at the peak of the temporal evolution of the reactive species. The distance to the plasma pencil is precisely measured by an adjustable micrometer.

The average plasma bullet velocity is calculated at the peaks of N_2^*, N_2^+, and He* temporal emissions as a function of the applied voltage. The launching time of the plasma bullet is determined by an ICCD camera, and then it is subtracted from the time of the highest peak in order to calculate the average plasma bullet velocity more accurately. It is found that the average plasma bullet velocity increases as the applied voltage increases (Fig. 9). In addition, identical average

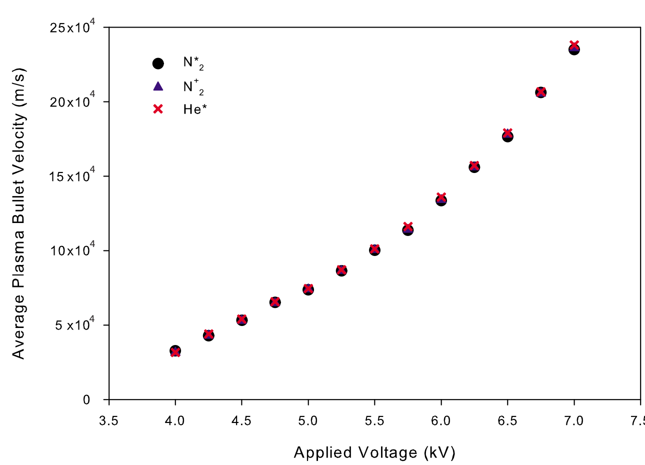

FIG. 9. (Color online) The average plasma bullet velocity for different reactive species as a function of the applied voltage (pulse width: 2000 ns; repetition rate: 5 kHz; flow rate: 5.0 l/min).

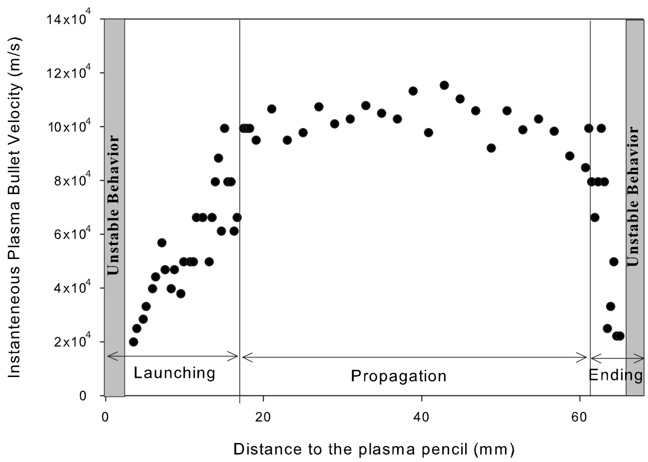

FIG. 10. The instantaneous plasma bullet velocity from the emission of SPS by a time-resolved OES (applied voltage: 5.5 kV; pulse width: 2000 ns; repetition rate: 5 kHz; flow rate: 5 l/min).

plasma bullet velocity is obtained from the emission of different reactive species for each applied voltage.

The instantaneous plasma bullet velocity is calculated from the consecutive temporal emissions of N_2^* (SPS) at 337.1 nm along the plasma jet since N_2^* (SPS) at 337.1 nm is one of the strongest emissions along the plasma jet. Each consecutive measurement is done by only one PMT (only the focal point is displaced by a micrometer). The oscilloscope output is averaged 500 times in order to obtain more accurate data. Therefore, the resolution of the oscilloscope allows decreasing the time error to 0.5 ns for each acquisition. As shown in Fig. 10, the instantaneous plasma bullet velocity does not follow a smooth velocity curve due to the highly collisional medium of air at atmospheric pressure. However, the numerous experimental observations show a consistent pattern. The instantaneous plasma bullet velocity experiences three different phases during its travel: launching, propagation, and ending (Fig. 10). The plasma bullet launches from the plasma pencil with relatively lower velocities, and then it reaches its maximum at 1.1×10^5 m/s. This increase is due to an excessive amount of nitrogen molecules in the air.[4] After that, the plasma bullet enters the propagation phase. During the propagation, its velocity remains almost constant. At the end of the pulse, the applied high voltage starts decreasing, and the plasma bullet comes to an end at around 70 mm in an abrupt manner. These three phases can be seen from the ICCD camera photographs in Fig. 11. It is worth noting that the velocity measurements at the early beginning and late ending of the propagation are unstable (gray regions in Fig. 10). In these regions, the plasma bullet is not propagating or seems to oscillate back and forth. For the early beginning, the reason of this instability is that the plasma bullet just starts being formed, and is still in contact with the reactor (i.e., the dielectric surface of the electrode). And, as stated in Ref. 4, air molecules start playing an important role in the plasma bullet propagation mechanism. For the late ending, as discussed in Ref. 9, the plasma bullet cannot sustain the chemical reactions due to quenching of excited states by air molecules after a certain spatial point. This quenching phenomenon causes the plasma emission to faint, undergoing electron attachment, and ion recombination at the end of the pulse. That point corresponds to the late ending of the plasma bullet propagation.

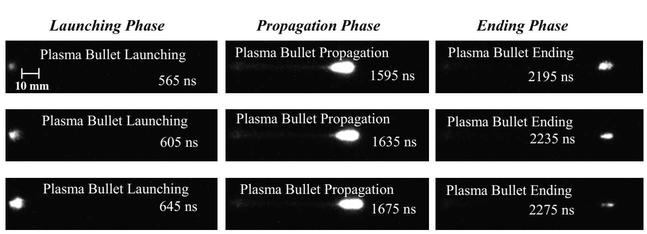

FIG. 11. Plasma bullet experiences three different phases: launching, propagation, and ending applied voltage: 5.5 kV; pulse width: 2000 ns; repetition rate: 5 kHz; flow rate: 5 l/min).

IV. CONCLUSION

The plasma bullet lifetime depends on the helium mole fraction along the ionization channel, the width of the applied voltage pulse and its magnitude, and the secondary discharge ignition time. The plasma bullet follows the trajectory of the helium gas channel, indicating that the helium mole fraction value along the ionization channel should be more than a critical limit to sustain the propagation. This critical value was determined in Ref. 9. The width of the applied voltage pulse is also important. For pulse widths less than a certain limit, the plasma bullet stops propagating just after the secondary discharge ignition, which occurs at the end of the applied voltage pulse. For longer pulses the diffusion of air into the helium channel extinguishes the plasma bullet before the arrival of the secondary discharge. In addition, how much energy is transferred into the ionization channel is an important parameter because the plasma bullet dissipates its energy as it propagates forward.

A new technique using time-resolved OES is employed for the accurate determination of the plasma bullet velocity. The velocity of the plasma bullet is an important parameter in order to understand its plasma bullet behavior. It is worth noting that this velocity is in the supersonic region without any externally applied electric field. It is found that the average plasma bullet velocity increases as the energy transferred into the ionization channel increases, and the different reactive species travel with similar velocities. Our previous results regarding the instantaneous plasma bullet velocity have been greatly improved by increasing the resolution of our measurements. This new high resolution enables us to observe a pattern along the plasma jet covering three different phases: launching, propagation, and ending.

ACKNOWLEDGMENTS

This work was supported by an AFOSR Grant No. FA9550–08–1–0487. The authors thank Julien Jarrige, a former research associate at Laser and Plasma Engineering Institute, Old Dominion University, for several useful discussions.

[1]M. Laroussi and T. Akan, Plasma Processes Polym. **4**, 777 (2007).
[2]M. Laroussi, IEEE Trans. Plasma Sci. **93**, 3813 (2009).
[3]X. Lu and M. Laroussi, J. Appl. Phys. **100**, 063302 (2006).

[4]N. Mericam-Bourdet, M. Laroussi, A. Begum, and E. Karakas, J. Phys. D: Appl. Phys. **42**, 055207 (2009).
[5]J. L. Walsh, F. Iza, N. B. Janson, V. J. Law, and M. G. Kong, J. Phys. D: Appl. Phys. **43**, 075201 (2010).
[6]Q. Xiong, X. Lu, J. Liu, Y. Xian, Z. Xiong, F. Zou, C. Zou, W. Gong, J. Hu, K. Chen, X. Pei, and Z. Jiang, J. Appl. Phys. **106**, 083302 (2009).
[7]Y. Sakiyama, D. B. Graves, J. Jarrige, and M. Laroussi, Appl. Phys. Lett. **96**, 041501 (2010).
[8]M. Laroussi, X. Lu, V. Kolobov, and R. Arslanbekov, J. Appl. Phys. **96**, 3028 (2004).
[9]E. Karakas, M. Koklu, and M. Laroussi, J. Phys. D: Appl. Phys. **43**, 155202 (2010).
[10]J. Shi, F. Zhong, J. Zhang, D. W. Liu, and M. G. Kong, Phys. Plasmas **15**, 013504 (2008).
[11]M. Teschke, J. Kedzierski, E. G. Finantu-Dinu, D. Korzec, and J. Engemann, IEEE Trans. Plasma Sci. **33**, 310 (2005).